A Mathematical Programming Approach for Allocation and Analysis of TCSC in Power Transmission Systems

J. S. Pereira, E. A. Belati, C. F. Nascimento, P. F. Silva and P. Rossoni

Abstract—**In this paper, a mathematical programming approach based on a branch and bound (B&B) algorithm is proposed in order to determine the optimal allocation of thyristor-controlled series compensators (TCSC) in electrical power transmission systems, considering line thermal limits. The TCSC modeling is added in the Y-bus matrix, facilitating the computational implementation. B&B-Y is the methodology used in this paper aiming to maximize the loading of the system considering a certain quantity of TCSC. In addition, the proposed algorithm is implemented for another test, using a determined number of TCSC, in order to improve the network voltage profile and minimize the total transmission losses. The methodology uses an interior point method to solve the problem relaxed, modeled as a reactive optimal power flow problem. Simulations are performed on the IEEE 118-bus test system, allocating different quantities of TCSC to find the maximum load the system can support. Given a certain number of TCSC, previously defined for a specific load, the TCSC are reallocated considering different objectives. For two TCSC the time for relocation is shorter than 4 seconds. The results also show that from three TCSC onwards, the maximum load increasing is not relevant, being around 0.3%. Therefore, the conclusion is that the algorithm has a low processing time, and conservative solutions allied with the presented methodology can be used in the optimal allocation of TCSC, what the aim is to optimize the system's performance.**

Index Terms—**Flexible AC transmission systems, Mathematical programming, Optimization, Power system control, Reactive power control, TCSC.**

I. Introduction

Throughout the years, electrical power systems have been enhancing their demand and limitation of energy resources, being forced to operate near their stability and load margins [1]. Distributed generation and reinforcement of transmission lines are both available solutions to avoid congestion and instability in the power system, but they have high costs and involve environmental issues. A widely considered alternative approach is the flexible AC transmission system (FACTS) [2]. These devices are based on power electronics and can regulate and control one or more parameters of the AC transmission system, such as bus voltage, line reactance, and phase angle [3].

J. S. Pereira, Federal University of ABC, was with Federal University of ABC, Santo André, Brazil, (e-mail: j.pereira@ufabc.edu.br).

E. A. Belati, Author is with Center for Engineering, Modeling and Applied Sciences (CECS), Federal University of ABC, Santo André, Brazil, (e-mail: edmarcio.belati@ufabc.edu.br).

C. F. Nascimento, Author is with Center for Exact Sciences and Technology (CCET),, Federal University of São Carlos, Brazil, (e-mail: claudionor@ufscar.br).

P. F. Silva, Author is with CCET, Federal University of São Carlos, Brazil, (e-mail: paulofs@estudante.ufscar.br).

P. Rossoni, Author is with CECS, Federal University of ABC, Santo André, Brazil, (e-mail: priscila.rossoni@ufabc.edu.br).

There are several types of FACTS and they might be classified according to their connection to the network, such as series, parallel, series-parallel, or series-series. Moreover, their benefits for the network depend on their type, as well as their quantity, size, and location.

This work proposes to apply the thyristor controlled serial compensator [4], [5]. The TCSC is connected in series to the transmission line and uses thyristor valves to control the line reactance, in order to control its power flow. The TCSC has influence on the system, enhancing the total transfer capability (TTC), improving voltage stability, reducing generation costs, and ameliorating security based on risk, besides other benefits [4].

A power system can operate safely and economically if its parameters are optimized. The optimal power flow (OPF) [6], [7] is widely used in the literature to optimize the power system and has variations that depend on the study objectives. One of these variations is the reactive optimal power flow (ROPF) that aims to optimize the network through the control of the reactive power injections available in the network and adjustment of other controls, such as the tap settings of the load tap changing (LTC) transformer [8]. The OPF can also be modeled to allocate devices, as proposed in this work - TCSC allocation. In this modeling, binary variables [9] must be included in the problem, representing the allocation (value 1) or no allocation (value 0) of a device in a network location.

The FACTS allocation problem is a mixed-integer nonlinear programming (MINLP) problem [9] and has been solved in the literature applying different techniques.

Heuristic and metaheuristics has been widely used for example in [10] to determine the optimal placement of the TCSC in order to obtain the lowest generation cost. In the paper, the author used differential evolution (DE) and compared the results using genetic algorithms (GAs). In [11] a method for decreasing power losses and voltage regulation by means of optimal locating and sizes of the reactive power compensators (SVC and TCSC) is proposed by means of Dynamic Programming (DP) and PSO algorithm. The hybrid tabu search and simulated annealing (TSSA) was used in [12] in order to locate TCSC and static var compensator (SVC) in the IEEE 118-bus test system to maximize load capacity and minimize transmission loss. The authors of [13] use the adaptive cuckoo search (ACS) metaheuristic to identify the optimal allocation of a TCSC in the IEEE 9-bus test system, in order to minimize transmission loss in this network, and compared the results with a particle swarm optimization (PSO) and GA. The PSO is also employed in [13] with the objective of finding locations and specification of TCSCs and the unified power flow controllers (UPFCs) in order to optimize the annual cost and the security of the power system studied, considering four different scenarios. Evolutionary strategy (ES) is employed by the authors of [14] to optimally allocate TCSCs in the IEEE 14-bus test system in order to minimize installation cost and maintain operational limits. In [15] the authors used the improved moth flame optimization (IMFO) technique for optimal location and specification of (TCSC) with the objective of reducing load shedding, preventing voltage collapse, and enhancing the power system load capacity. A cuckoo search (CS) metaheuristic is used in [16] for best locations of single and multi-type FACTS device. A metaheuristic approach named grey wolf optimizer (GWO) is used, considering a multi-objective task, for optimum tuning of TCSC [17]. In [18] is used a GA for the optimum setting of TCSC. The whale optimization algorithm (WOA) is used for the optimal setting of TCSC and SVC in [19]. A chemical reaction optimization (CRO) is a relatively new metaheuristic technique which is applied in [20] for optimal allocation of SVC and TCSC. In [5] the authors investigated the influence of switching losses on the optimum allocation of the TCSC in power systems, using a Multi-Objective optimization technique. An optimization algorithm, Multi-Objective Artificial Bee Colony (MOABC) was used in the solution process. An implementation of chaotic immune symbiotic organisms search (CISOS) is used to solve optimal TCSC allocation problem in [21]. As noted in the consulted bibliography, many studies use metaheuristics. However, due to the stochastic characteristic of the metaheuristics, the optimal solution cannot be guaranteed, as well as a conservative solution.

Some authors explore the mathematical programming, such as the authors of [22] who use a Benders decomposition approach to find the optimal location and setting of TCSCs in the IEEE 118-bus test system in order to minimize the generation cost and investment cost of installing of the TCSCs. In [23] is proposed a methodology for TCSC planning using mixed integer programming (MIP) in order to improve the voltage profile, as well as minimize the investment and maximize the system load capacity.

In this paper, a B&B algorithm was used to allocate several TCSC. The modeling modifies the Y-bus matrix, where the binary variables are added. The B&B algorithm uses the interior point method to solve the ROPF problem, aiming maximum load capacity that is distributed equally between all load buses of the system. The methodology is identified in this work as B&B-Y. Thereafter, the executed simulation obtained through the B&B-Y is compared to the hybrid TSSA and evolutionary programming (EP) algorithms [12], demonstrating the B&B-Y quickness. Finally, a predicted overload is considered in the system and the B&B-Y runs again to allocate TCSC in order to analyze different scenarios with different considerations in the objective function.

Therefore, the main contribution of this paper is the modeling of the problem, which represents the binary variables in the Y-bus matrix, and the heuristic of optimization, which consists of verifying the maximum load capacity in relation to the quantity of TCSCs, and then analyze the system with different objectives. This heuristic modeling makes feasible the use of B&B algorithm, which can be confirmed based on the results presented.

The rest of this paper is organized as follows: Section II presents the TCSC and its expression applied in the ROPF formulated. Section III describes the ROPF problem. Section IV presents the methods used to solve the MINLP problem created. Section V provides computational results and discussion on implementing in the IEEE 118-bus test systems considering line thermal limits. Finally, some concluding remarks are offered in Section VI.

II. Thyristor Controlled Series Compensator

The TCSC, represented in Fig. 1, is a FACTS device, which is basically composed of a fixed series capacitor, C, in parallel with a thyristor-controlled reactor (TCR). The TCR is composed of a reactor, L, controlled by antiparallel thyristor pair, T_1 and T_2, which have the function of controlling the current injected in the line. This is the basic concept of TCSC, disregarding any protective equipment [24], [25].

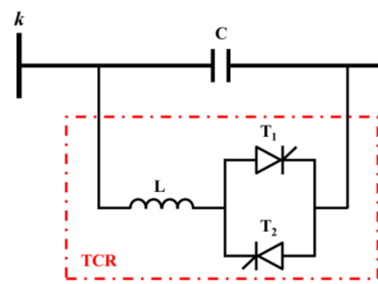

Fig. 1. Basic one-line diagram of TCSC.

A TCSC is inserted in the transmission line in order to control the effective reactance of the line, what is composed of the characteristic reactance of the line plus the TCSC reactance. A diagram of the line with TCSC located is presented in Fig. 2.

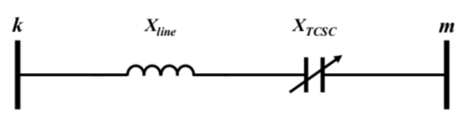

Fig. 2. Basic one-line diagram of transmission line with TCSC located.

The Fig. 2 is converted into the equation showed below:

$$X_{km} = X_{line_{km}} + \beta_{km}.X_{TCSC_{km}} \quad (1)$$

where β_{km} is the binary variable that defines the line where the TCSC is allocated considering the following:

$$\begin{cases} \beta_{km} = 0, \text{TCSC is not allocated in the line from bus } k \text{ to } m. \\ \beta_{km} = 1, \text{TCSC is allocated in the line from bus } k \text{ to } m. \end{cases}$$

The admittance matrix used to calculate the power flow [26] contains information about the network elements, such as lines, transformers, compensators, etc.

Therefore, (2) and (3), respectively, represent the conductance and susceptibility of the line formulated in the algorithm, to introduce the TCSC information in the Y-bus matrix.

$$g_{km} = \frac{R_{line_{km}}}{R_{line_{km}}{}^2 + \left(X_{line_{km}} + \beta_{km} X_{TCSC_{km}}\right)^2} \quad (2)$$

$$b_{km} = \frac{-\left(X_{line_{km}} + \beta_{km} X_{TCSC_{km}}\right)}{R_{line_{km}}{}^2 + \left(X_{line_{km}} + \beta_{km} X_{TCSC_{km}}\right)^2} \quad (3)$$

where g_{km} is the line conductance from bus k to bus m; b_{km} is the line susceptance from bus k to bus m; and $R_{Line_{km}}$ is the line resistance from bus k to bus m.

In addition, TCSC compensation is limited due to its intrinsic characteristic. The TCSC reactance is calculated as represented in (4).

$$X_{TCSC} = \alpha_{TCSC} . X_{line} \quad (4)$$

where α_{TCSC} is the degree of compensation by TCSC.

This paper considers a work range of a TCSC α_{TCSC} from - 0.7 to 0.2 [27].

This formulation introduces the variables β_{km} (binary) and α_{TCSC} (continuous) in the Y-bus matrix, which are optimized in the process.

III. Reactive Optimal Power Flow

ROPF is a specific problem related to FPO, where all active power generation are fixed, except the swing bus. The injections of reactive power are adjusted by devices with reactive generation available, and other network controls, such as taps of transformers. In addition to this model, the TCSC reactances are controlled too. The problem also considers the TCSC allocation, making it a MINLP problem, as described by (5) - (13).

$$max\ F \quad (5)$$

Subjected to

$$P_{g_k} - P_{L_k} - V_k \sum_{m \in \kappa} V_m (G_{km} cos\theta_{km} + B_{km} sin\theta_{km}) = 0 \quad (6)$$

$$Q_{g_k} + Q_k^{sh} - Q_{L_k} - V_k \sum_{m \in \kappa} V_m (G_{km} sin\theta_{km} - B_{km} cos\theta_{km}) = 0 \quad (7)$$

$$V_k^{min} \leq V_k \leq V_k^{max} \quad (8)$$

$$\alpha_{TCSC}^{min} . X_{line} \leq X_{TCSC} \leq \alpha_{TCSC}^{max} . X_{line} \quad (9)$$

$$Q_{g_k}^{min} \leq Q_{g_k} \leq Q_{g_k}^{max} \quad (10)$$

$$P_{th_{km}}^{min} \leq P_{km} \leq P_{th_{km}}^{max} \quad (11)$$

$$n_{TCSC} = \sum \beta_{km} \quad (12)$$

$$\beta_{km} = 0\ or\ 1 \quad (13)$$

where F is the objective function; P_{gk} is the active output of the generating units in the bus k; Q_{gk} is the reactive output of the generating units in the bus k; Q_k^{sh} is reactive power injection due to shunt elements in the bus k. P_{L_k} is the active power consumed in the bus k; Q_{L_k} is the reactive power consumed in the bus k; V_k is the voltages in the bus k; V_m is the voltages in the bus m; G_{km} is the real element of the admittance matrix element; B_{km} is the imaginary element of the admittance matrix element; θ_{km} is the phase angle between bus k and bus m; V_k^{min} is the minimum voltage limit; V_k^{max} is the maximum voltage limit; $Q_{g_k}^{min}$ is the minimum reactive outputs of the generating units in the bus k; $Q_{g_k}^{max}$ is the maximum reactive outputs of the generating units in the bus k; $P_{th_{km}}^{min}$ is the minimum line thermal limit in the line from k to m; $P_{th_{km}}^{max}$ is the maximum line thermal limit in the line from k to m; P_{km} is the active power flow in the line from k to m; and n_{TCSC} is the amount of TCSC available to be allocated.

1.1. Objective Function

The problem objective is to maximize the system load capacity, improve the voltage profile at 1 pu, and minimize the total active power loss. This situation is formulated as multi-objective optimization problems, also called of multicriteria, multiperformance or vector optimizations [28]. Therefore, (5) is calculated as:

$$F = w_1 \sum_{k=1}^{NB} S_{L_k} + w_2 \sum_{k=1}^{NB} (1 - V_k)^2 + w_3 \sum_{i=1}^{NL} g_{km} (V_k^2 + V_m^2 - 2 V_k V_m cos\theta_{km}) \quad (14)$$

where g_{km} is the conductance of the $k - m$ line; NB is the total number of busses in the network; NL is the total number of lines in the network i; w_1, w_2, w_3 are the weight constants; and S_{L_k} is the apparent power consumed in the bus k. The final active and reactive powers consumed in each bus are calculated through an overload factor that is multiplied by the nominal active (P_{L0_k}) and reactive (Q_{L0_k}) load, maintaining the load power factor.

$$P_{L_k} = \delta P_{L0_k} \quad (15)$$

$$Q_{L_k} = \delta Q_{L0_k} \quad (16)$$

where δ is the overload factor. This overload factor is used in order to demonstrate the overload supported by the network.

1.2. Variables

The variables of this problem can be divided into two sets, called controlled variables and control variables. Controlled variables describe the system response to changes in control variables, such as voltage magnitude in load buses and currents in transmission lines. On the other hand, the control variables can be adjusted to find the optimal solution problem. The control variables are, for example, the voltage magnitude of the generator buses, the reactivity power of the generator units, the reactance of the TCSC, and the binary variable that represents TCSC allocation.

1.3. Equality Constrains

The equality constraints are the system power balance equation at each node [26], as represented in (6) and (7).

1.4. Inequality Constrains

The inequality constraints are the physical and operational limits of the system. This paper considered a permitted variation of ±6% in the voltage magnitude for each bus, the degree of compensation by TCSC, limits of the reactive power of generating units, line thermal limits [29], the amount of TCSC, the binary variable and the tap settings of the LTC transformers.

IV. Computational Tools

The problem purposed is implemented in AMPL programming language [30] and solved through the solver Knitro [31], [32], which provides different methods to solve MINLP problems.

In this paper, the optimization problem is solved through B&B algorithm with the use of an interior point (IP) method. The Knitro offers a nonlinear B&B method. The B&B method is primarily designed for convex models, but it can also be applied to non-convex models. In this case, it may sometimes get stuck at integer feasible points that are not globally optimal solutions when the model is nonconvex. Thus, there is no guarantee that the solution found is the global optimal. To minimize this deficiency, the solver works with various search strategies involving B&B, which can be chosen automatically by the solver, depending on the size and characteristics of the problem. Several algorithmic options to solve the non-linear programming problem are available at Knitro [31]. In this paper, the IP method was used, which will be used in the solution of the B&B subproblems. An overview of the IP and B&B methods is presented in sequence.

A. Overview of Interior Point Method

The interior point method is also known as a barrier method [32], [33]. The problem solved by this method has the form:

Minimize

$$f(x,y) - \mu \sum ln\, s$$

Subjected to

$$h(x,y) = 0 \quad g(x,y) - s = 0 \tag{17}$$

where $x \in \mathbb{R}^n$, y is binary, $\mu > 0$, s slack variables, $f(x)$ represents the objective function and $h(x)$ and $g(x)$ represent the equality and inequality constraints, respectively.

The algorithm consists of finding solutions of the barrier problem in (17), using trust regions and a merit function to promote convergence. The solving process is repeated until the solution reaches the desired accuracy, decreasing the barrier parameter for each sub-problem. In order to solve the barrier problem (17) considering a determined barrier parameter, a Lagrangian function in (18) is associated to this function. λ and π are the Lagrange multipliers.

$$\begin{aligned} L(x,y,s,\lambda,\pi) = f(x,y) - \mu \sum ln\, s \\ - \lambda \sum ln\, h(x,y) \\ - \pi \sum ln(g(x,y) - s) \end{aligned} \tag{18}$$

Then, (18) has to state the first order necessary optimality conditions, as showed in (19), also called Karush-Kuhn-Tucker (KKT) conditions.

$$\nabla L(x,y,s,\lambda,\pi) = 0 \tag{19}$$

Every new step is iterated by solving the primal-dual KKT matrix using direct linear algebra [31] [32].

B. Overview of Branch and Bound Algorithm

The B&B method was developed in the 1960s [34] for application to discrete and combinatorial optimization problems and it is widely used to solve integer linear programming (ILP) problems. The prerogative of B&B is to explore a research space through a tree search until the optimal solution to the problem is found.

In the B&B for a binary searching, this method is initialized with a continuous relaxing of the problem. Considering $(x^{**}; y^{**})$ a feasible solution and y^{**} is equal to 0 or 1, then it is the first incumbent solution (I). If $(x^{*}; y^{*})$ a feasible solution but y^{*} is not binary, then the problem must be divided into sub-regions, creating sub-problems called nodes.

Maximize

$$f(x,y)$$

Subjected to

$$\begin{aligned} h(x,y) = 0 \\ g(x,y) \geq 0 \\ \mathrm{x}^{\min} \geq \mathrm{x} \geq \mathrm{x}^{\max} \\ \mathrm{y} \geq 0 \end{aligned} \tag{20}$$

and

Maximize

$$f(x,y)$$

Subjected to

$$\begin{aligned} h(x,y) = 0 \\ g(x,y) \geq 0 \\ x^{min} \geq x \geq x^{max} \\ y \leq 1 \end{aligned} \tag{21}$$

If a problem solution is infeasible, then it is called sounded (*S*). If a problem solution is feasible and y is binary, then it has two results: a) if it is worse than $(x^{**}; y^{**})$, then the solution is *S*; else b) it is the new *I* $(x^{**}; y^{**})$ and then the old *I* becomes *S*. Otherwise, the problem is divided into sub regions again, continuing the programming until *I* is found through the B&B Tree created by this entire process [35]. Fig. 3 presents the flowchart based on B&B algorithm.

The performance of the B&B algorithm is related to the search strategy (SS) used. In [36], several strategies are presented, such as depth-first search (DFS), breadth-first search (BrFS), best-bound search (BBS) and cyclic best-first search (CBFS) strategy that is a generalization of these three. Another key point in a B&B algorithm is the definition of the branch strategy (BS), what determines how the subproblems will be divided. There are some strategies, such as binary branching (BB) [36], wide branching (WB) [36], pseudocost branching (PCB) [37], most fractional (MF) [38], strong branching (SB) [38], among others. The choice of both SS and BS was automatically defined by the Knitro solver, who makes the decision based on the problem characteristics.

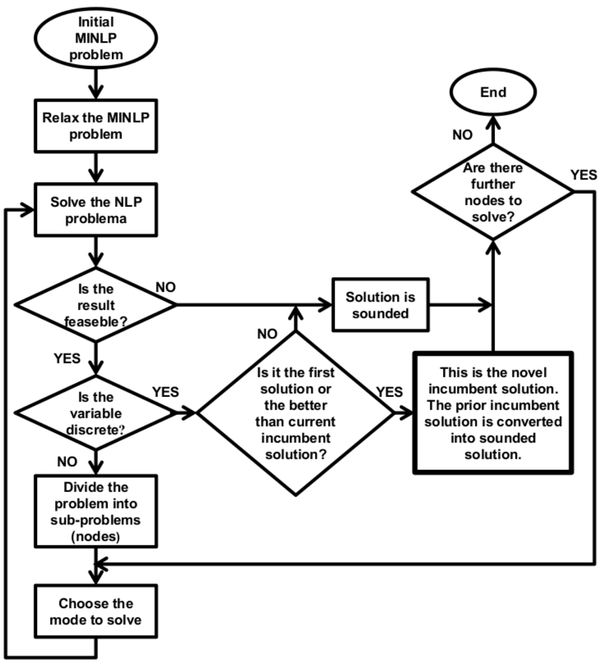

Fig. 3. Flowchart based on B&B algorithm.

V. Case Study

The model is tested and evaluated using a modified IEEE 118-bus system, in order to demonstrate the applicability of the proposed procedure. The network data for the 118-bus is available in [39] and the line thermal limits used are in Appendix (Table A), found in [40]. This network has 179 sections, 9 of which are transformers and 170 candidate transmission lines for device allocation. The LTC transformer tap is assumed to be set to 1. The power system includes 54 thermal units. Bus 69 is the slack system bus. The total grid load for the nominal case is 4,242 MW and 1,438 Mvar, referring to active and reactive power, respectively.

The problem was implemented in AMPL, using the Knitro solver. The simulations were performed using an Intel Core i5-5200U 1000GB HDD personal computer with an installed memory (RAM) of 4GB on a Microsoft Windows 10 64-bit operating system.

A. Maximum Load Capacity

The analysis methodology initially consists of run the ROPF to find the maximum load capacity supported by the network in relation to the quantity of TCSC available for allocation. The weight constants of the target function (14) used are $w_1 = 1$, $w_2 = 0$ and $w_3 = 0$. The results obtained in this analysis are shown in Fig. 4.

In this case, there is an expressive overload increasing when the firsts three TCSC are allocated in the network, as shown in Fig 4. From three allocated TCSCs there are no major contributions, indicating that three is an acceptable value. Furthermore, the maximum overload tolerated by the system is 1.226 pu, i.e., total active and reactive loads of up to 5,200.7 MW and 1,763.0 Mvar, respectively.

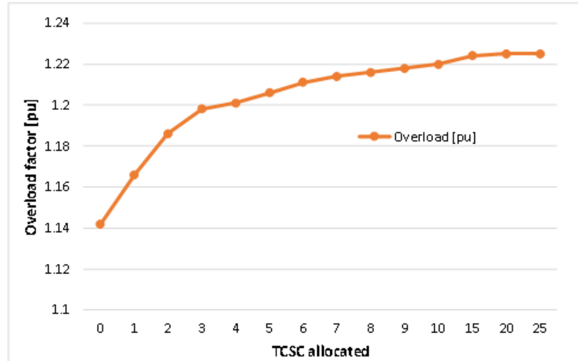

Fig. 4. Overload factor and B&B nodes numbers versus amount of TCSC allocated in the system.

The B&B-Y performance is presented in the Table I. The results demonstrate that the quantity of TCSC available to be allocated is not proportional to the run time of the program, as well as it is not linked to the B&B Tree dimension.
In this paper, the computational performance obtained in the Table I (for 2 TCSCs) was compared with the results obtained in [11]. However, EP obtained the performance in [11] and Hybrid TSSA, considering the same operating conditions used in this work. Note that the results in Table I presents an execution time 1,802.79 seconds faster than Hybrid TSSA and 2,412.99 seconds faster than EP. The authors of [12] also consider the weight constants in (14) as being $w_1 = 1$, $w_2 = 0$ and $w_3 = -1$, but the overload is applied unequally only in load buses and the active power generation is distributed through every generation buses, respecting their limits.

TABLE I
PROGRAMMING PERFORMANCE PER TCSC AMOUNT

TCSC Qty	Total Nodes	CPU Time [s]	Overload [pu]
0	-	-	1.142
1	3	2.19	1.166
2	5	3.81	1.186
3	48	31.09	1.198
4	115	104.45	1.201
5	105	98.33	1.206
6	163	158.00	1.211
7	150	181.42	1.214
8	59	138.53	1.216
9	462	730.27	1.218
10	4554	6,137.19	1.220
15	1301	1,971.98	1.224
20	2103	3,963.39	1.225
25	17463	3,1356.48	1.225

B. Planning System Overload

The system without any FACTS device supports an overload up to 1.142 pu. However, planning an increase in consumption up to 17.5% in the network, at least two TCSC are necessary with the aim of supporting such overload, respecting the operational limits, since only one TCSC supports an increase of up to 16.6%.

This initial analysis is important for the system planner to know the system's capacity as a function of the number of TCSC, and from there, evaluate the best place to allocate the TCSC in terms of the defined operational objectives.

Therefore, two TCSC must be available to support 17.5% overload. With the purpose of taking advantage of the available FACTS and improve the network, the weight constants in the objective function (14) can be changed to reallocate the TCSC. Table II presents some system parameters for the different allocations simulated so far, where:

a) **Case 1**: $w_1 = 1$, $w_2 = 0$ and $w_3 = 0$ (seeks maximum loading, presents in the item A);
b) **Case 2**: $w_1 = 0$, $w_2 = -1$ and $w_3 = 0$ (seeks the minimum voltage deviation in relation to 1 pu);
c) **Case 3**: $w_1 = 0$, $w_2 = 0$ and $w_3 = -1$ (seeks the minimum active loss in the system);
d) **Case 4**: $w_1 = 0$, $w_2 = -0.95$ and $w_3 = -0.05$ (seeks a balance between minimum voltage deviation and active losses).

The values of w_2 and w_3 were obtained experimentally searching a balance between the objectives.

Table II shows that both cases have one TCSC allocated in the line 69-77 with inductive effect, in order to limit the power flow on this line.

This is the most critical line in thermal limit, as shown in Table III, which ranks from highest to lowest value of the first three Lagrange multipliers [41], π, when optimizing the system without FACTS devices [42], [43]. This means that this line is the most susceptible to variation of the objective function when their parameters are changed.

Case 2 considers only minimizing the voltage deviation. As can be seen in the last column, the sum of the voltage deviation is the smallest for case 2 (1.2004 pu). Case 3 considers only the minimization of losses, with a value of 233 MW. Depending on the objective, the allocation of the TCSC can be different, what validates the algorithm. Case 4 presents an equilibrium regarding the minimization of voltage deviation and active losses, what can be a good alternative, since the allocation the TCSC coincides with case 3.

Regarding allocations, all the lines chosen are connected to the slack bus, the only bus with active generation available in the study.

TABLE II.
SYSTEM PARAMETERS WITH 2 TCSC ALLOCATED, CONSIDERING DIFFERENT WEIGHT CONSTANTS IN THE OBJECTIVE FUNCTION

Cases	Allocation [from-to]	α_{TCSC}	δ	Total Active Loss	Total Voltage Deviation
1	69-75	-0.70	1.186 pu	281 MW	3.3150 pu
	69-77	0.20			
2	69-75	-0.61	1.175 pu	264 MW	1.2004 pu
	69-77	0.20			
3	69-70	-0.60	1.175 pu	233 MW	4.4478 pu
	69-77	0.20			
4	69-70	-0.70	1.175 pu	254 MW	1.2804 pu
	69-77	0.20			

TABLE III
LAGRANGE MULTIPLIER

Line [from to]		π
69	77	4.87370373862
23	32	0.00000003256
68	69	0.00000002142

The Case 2 allocates the TCSC in the line 69-75, since the bus 75 presents the biggest voltage deviation where the voltage is equal to 0.9713 pu, so the device allocated in this line is used to increase the voltage and make it closer to 1 pu. The Fig. 5 illustrates the voltage in the buses connected to the slack bus.

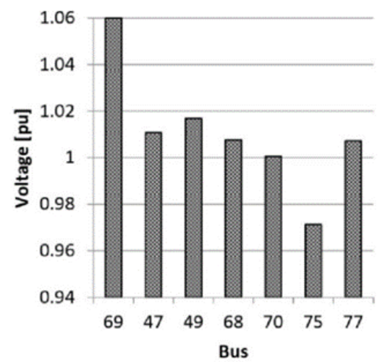

Fig. 5. Overload factor versus amount of TCSC allocated in the system.

Cases 3 and 4 have TCSC allocated in the line 69-70, as this line limits more power flowing through the line and leads to less power loss than placing TCSC in the line 69-75. However, the control of TCSCs reactance in the Case 3 is reduced with the aim of decreasing the total power loss, by diminishing the power flow in this line. The Fig. 6 illustrates the power flows in some transmission lines, as well as their limits in the Cases 3 and 4. The losses are presented in the Table IV.

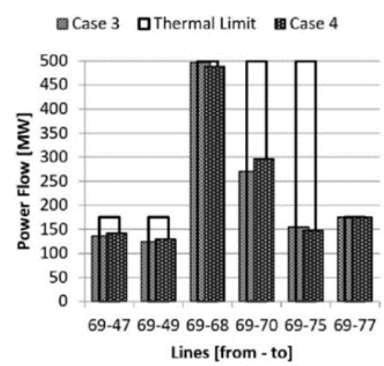

Fig. 6. Power flow and thermal limit in each line

TABLE IV
TRANSMISSION LOSSES

Lines [from-to]	Losses [MW] Case 3	Case 4
69-47	14.0	15.1
69-49	13.6	14.6
69-68	0.0	0.0
69-70	19.6	23.6
69-75	8.8	8.2
69-77	8.5	8.6

VI. Conclusion

In this paper, a mathematical programming approach based on alternative modeling of the Y-bus matrix with a B&B algorithm was proposed to determine the optimal location of TCSC, considering the thermal limits of the line. The problem was modeled with a ROPF and applied to the IEEE 118-bus test system. First, the ROPF is solved considering the objective function of maximizing the system load capacity by allocating different quantities of devices in the network. This simulation results showed the relationship between increased transmission capacity and the amount of TCSC, highlighting the importance of this analysis due to the costs related to the equipment. Subsequently, two TCSC are allocated considering in addition to the initial scenario, three more scenarios, with different weight constants in the objective function. The simulation results illustrate the importance of controlling the reactance of the TCSC. The TCSC with inductive effect can be used to limit the power that flows in the overloaded lines; otherwise, the TCSC with capacitive effect can be used to improve the power that flows in the line with more availability. The performance of B&B-Y is compared to TSSA hybrid technique and EP algorithm, showing the good yield of the B&B-Y algorithm for the problem formulated. For future work, we suggest implementing a formulation that considers the dispatch of the active and reactive powers of the generators and the cost of the TCSC, with the objective of minimizing the costs involved and maximizing the loading of the system.

Appendix

Table A
Line thermal limits used of 118-bus system.

k	*m*	MW	*k*	*m*	MW	*k*	*m*	MW
1	2	175	44	45	175	68	81	500
1	3	175	45	46	175	80	81	500
4	5	500	46	47	175	77	82	200
3	5	175	46	48	175	82	83	200
5	6	175	47	49	175	83	84	175
6	7	175	42	49	175	83	85	175
8	9	500	45	49	175	84	85	175
5	8	500	48	49	175	85	86	500
9	10	500	49	50	175	86	87	500
4	11	175	49	51	175	85	88	175
5	11	175	51	52	175	85	89	175
11	12	175	52	53	175	88	89	500
2	12	175	53	54	175	89	90	500
3	12	175	49	54	175	90	91	175
7	12	175	54	55	175	89	92	500
11	13	175	54	56	175	91	92	175
12	14	175	55	56	175	92	93	175
13	15	175	56	57	175	92	94	175
14	15	175	50	57	175	93	94	175
12	16	175	56	58	175	94	95	175
15	17	500	51	58	175	80	96	175
16	17	175	54	59	175	82	96	175
17	18	175	56	59	175	94	96	175
18	19	175	55	59	175	80	97	175
19	20	175	59	60	175	80	98	175
15	19	175	59	61	175	80	99	200
20	21	175	60	61	500	92	100	175
21	22	175	60	62	175	94	100	175
22	23	175	61	62	175	95	96	175
23	24	175	59	63	500	96	97	175
23	25	500	63	64	500	98	100	175
25	26	500	61	64	500	99	100	175
25	27	500	38	65	500	100	101	175
27	28	175	64	65	500	92	102	175
28	29	175	49	66	500	101	102	175
17	30	500	62	66	175	100	103	500
8	30	175	62	67	175	100	104	175
26	30	500	65	66	500	103	104	175
17	31	175	66	67	175	103	105	175
29	31	175	65	68	500	100	106	175
23	32	140	47	69	175	104	105	175
31	32	175	49	69	175	105	106	175
27	32	175	68	69	500	105	107	175
15	33	175	69	70	500	105	108	175
19	34	175	24	70	175	106	107	175
35	36	175	70	71	175	108	109	175
35	37	175	24	72	175	103	110	175
33	37	175	71	75	175	109	110	175
34	36	175	71	73	175	110	111	175
34	37	500	70	74	175	110	112	175
37	38	500	70	75	175	17	113	175
37	39	175	69	75	500	32	113	500
37	40	175	74	75	175	32	114	175
30	38	175	76	77	175	27	115	175
39	40	175	69	77	175	114	115	175
40	41	175	75	77	175	68	116	500
40	42	175	77	78	175	12	117	175
41	42	175	78	79	175	75	118	175
43	44	175	77	80	500	76	118	175
34	43	175	79	80	175			

Acknowledgment

This work was supported in part by the FAPESP under Grants 2018/03015-2, 2014/14361-8 and 2016/08645-9, CNPq under Grants 306243/2014-8 and 305266/2018, FAPERJ under Grants E-26/202886/2017, E-26/101953/2012 and E-26/110400/2014, INERGE and CAPES.

References

[1] E. Ghahremani and I. Kamwa, "Optimal Placement of Multiple-Type FACTS Devices to Maximize Power System loadability using a generic graphical user interface," *IEEE Trans. Power Syst.*, vol. 28, no. 2, pp. 764–778, 2013.

[2] R. N. Diniz Costa Filho and V. L. Paucar, "Robust and Coordinated Tuning of PSS and FACTS-PODs of Interconnected Systems Considering Signal Transmission Delay Using Ant Lion Optimizer," *J. Control. Autom. Electr. Syst.*, vol. 29, no. 5, pp. 625–639, 2018.

[3] M. Karami, N. Mariun, and M. Z. A. A. Kadir, "On basic definition of optimal allocation of FACTS devices in power system," in *2009 IEEE Student Conference on Research and Development (SCOReD)*, 2009, pp. 418–421.

[4] V. Mahajan, "Thyristor Controlled Series Compensator," in *2006 IEEE International Conference on Industrial Technology*, 2006, pp. 182–187.

[5] M. Gitizadeh, H. Khalilnezhad, and R. Hedayatzadeh, "TCSC allocation in power systems considering switching loss using MOABC algorithm," *Electr. Eng.*, vol. 95, no. 2, pp. 73–85, 2013.

[6] E. C. Baptista, E. A. Belati, and G. R. M. Da Costa, "Logarithmic barrier-augmented Lagrangian function to the optimal power flow problem," *Int. J. Electr. Power Energy Syst.*, vol. 27, no. 7, 2005.

[7] A. L. L. Murari *et al.*, "Study of transmission system with wind power control and Optimal Reactive Power Flow," *Prz. Elektrotechniczny*, vol. 90, no. 7, 2014.

[8] Z. Yang, H. Zhong, A. Bose, Q. Xia, and C. Kang, "Optimal Power Flow in AC–DC Grids With Discrete Control Devices," *IEEE Trans. Power Syst.*, vol. 33, no. 2, pp. 1461–1472, 2018.

[9] M. Khanabadi, H. Ghasemi, and M. Doostizadeh, "Optimal Transmission Switching Considering Voltage Security and N-1 Contingency Analysis," *IEEE Trans. Power Syst.*, vol. 28, no. 1, pp. 542–550, 2013.

[10] B. Sookananta, "Determination of FACTS placement using differential evolution technique," in *2009 International Conference on Electrical Engineering and Informatics*, 2009, vol. 02, pp. 672–675.

[11] S. Shojaeian, E. S. Naeeni, M. Dolatshahi, and H. Khani, "A PSO-DP based method to determination of the optimal number, location, and size

of FACTS devices in power systems," *Adv. Electr. Comput. Eng.*, vol. 14, no. 1, pp. 109–114, 2014.

[12] S. Chansareewittaya and P. Jirapong, "Total transfer capability enhancement with optimal number of FACTS controllers using hybrid TSSA," in *2012 Proceedings of IEEE Southeastcon*, 2012, pp. 1–7.

[13] M. Taleb, A. Salem, A. Ayman, and M. A. Azma, "Optimal allocation of TCSC using adaptive cuckoo search algorithm," in *2016 Eighteenth International Middle East Power Systems Conference (MEPCON)*, 2016, pp. 387–391.

[14] D. Shchetinin and G. Hug, "Optimal TCSC allocation in a power system for risk minimization," in *2014 North American Power Symposium (NAPS)*, 2014, pp. 1–6.

[15] F. Sayed, S. Kamel, M. A. Taher, and F. Jurado, "Enhancing power system loadability and optimal load shedding based on TCSC allocation using improved moth flame optimization algorithm," *Electr. Eng.*, 2020.

[16] S. S. Akumalla, S. Peddakotla, and S. R. A. Kuppa, "A Modified Cuckoo Search Algorithm for Improving Voltage Profile and to Diminish Power Losses by Locating Multi-type FACTS Devices," *J. Control. Autom. Electr. Syst.*, vol. 27, no. 1, pp. 93–104, 2016.

[17] M. Rambabu, G. V. Nagesh Kumar, and S. Sivanagaraju, "Optimal Power Flow of Integrated Renewable Energy System using a Thyristor Controlled SeriesCompensator and a Grey-Wolf Algorithm," *Energies*, vol. 12, no. 11, p. 2215, Jun. 2019.

[18] D. L. Pravallika and B. V. Rao, "Flower Pollination Algorithm Based Optimal Setting of TCSC to Minimize the Transmission Line Losses in the Power System," *Procedia Comput. Sci.*, vol. 92, pp. 30–35, 2016.

[19] S. Raj and B. Bhattacharyya, "Optimal placement of TCSC and SVC for reactive power planning using Whale optimization algorithm," *Swarm Evol. Comput.*, vol. 40, pp. 131–143, 2018.

[20] S. Dutta, S. Paul, and P. K. Roy, "Optimal allocation of SVC and TCSC using quasi-oppositional chemical reaction optimization for solving multi-objective ORPD problem," *J. Electr. Syst. Inf. Technol.*, vol. 5, no. 1, pp. 83–98, 2018.

[21] M. K. Mohamad Zamani *et al.*, "Optimal TCSC Allocation via Chaotic Immune Symbiotic Organisms Search for Voltage Profile Improvement," *E3S Web Conf.*, vol. 152, 2020.

[22] O. Ziaee and F. F. Choobineh, "Optimal Location-Allocation of TCSC Devices on a Transmission Network," *IEEE Trans. Power Syst.*, vol. 32, no. 1, pp. 94–102, 2017.

[23] G. Y. Yang, G. Hovland, R. Majumder, and Z. Y. Dong, "TCSC Allocation Based on Line Flow Based Equations Via Mixed-Integer Programming," *IEEE Trans. Power Syst.*, vol. 22, no. 4, pp. 2262–2269, 2007.

[24] R. M. Mathur and R. K. Varma, "Index," in *Thyristor-Based FACTS Controllers for Electrical Transmission Systems*, IEEE, 2002, pp. 493–495.

[25] E. Acha, C. R. Fuerte-Esquivel, H. Ambriz-Pérez, and C. Angeles-Camacho, *FACTS: Modelling and Simulation in Power Networks*. Wiley, 2004.

[26] H. W. Dommel and W. F. Tinney, "Optimal Power Flow Solutions," *IEEE Trans. Power Appar. Syst.*, vol. PAS-87, no. 10, pp. 1866–1876, 1968.

[27] L. J. Cai, I. Erlich, and G. Stamtsis, "Optimal choice and allocation of FACTS devices in deregulated electricity market using genetic algorithms," in *IEEE PES Power Systems Conference and Exposition, 2004.*, 2004, pp. 201–207 vol.1.

[28] L. S. de Oliveira and S. F. P. Saramago, "Multiobjective optimization techniques applied to engineering problems," *J. Brazilian Soc. Mech. Sci. Eng.*, vol. 32, no. 1, pp. 94–105, Mar. 2010.

[29] G. C. Ejebe, J. Tong, J. G. Waight, J. G. Frame, X. Wang, and W. F. Tinney, "Available transfer capability calculations," *IEEE Trans. Power Syst.*, vol. 13, no. 4, pp. 1521–1527, 1998.

[30] B. W. K. Robert Fourer, David M. Gay, *AMPL: A Modeling Language for Mathematical Programming*. THOMSON, 2003.

[31] R. H. Byrd, J. Nocedal, and R. A. Waltz, "Knitro: An Integrated Package for Nonlinear Optimization BT - Large-Scale Nonlinear Optimization," G. Di Pillo and M. Roma, Eds. Boston, MA: Springer US, 2006, pp. 35–59.

[32] "User guide — Artelys Knitro 12.3 User's Manual." [Online]. Available: https://www.artelys.com/docs/knitro/2_userGuide.html. [Accessed: 11-Jan-2021].

[33] V. A. De Sousa, E. C. Baptista, and G. R. M. Da Costa, "Optimal reactive power flow via the modified barrier Lagrangian function approach," *Electr. Power Syst. Res.*, vol. 84, no. 1, pp. 159–164, 2012.

[34] A. H. Land and A. G. Doig, "An automatic method of solving discrete programming problems," *Econometrica*, vol. 28, no. 3, p. 497, 1960.

[35] D. T. Phan, "Lagrangian Duality and Branch-and-Bound Algorithms for Optimal Power Flow," *Oper. Res.*, vol. 60, no. 2, pp. 275–285, Apr. 2012.

[36] D. R. Morrison, S. H. Jacobson, J. J. Sauppe, and E. C. Sewell, "Branch-and-bound algorithms: A survey of recent advances in searching, branching, and pruning," *Discret. Optim.*, vol. 19, no. 3, pp. 79–102, 2016.

[37] M. Benichou, J. Gauthier, P. Girodet, G. Hentges, G. Ribière, and O. Vincent, "Experiments in mixed-integer linear programming," *Math. Program.*, vol. 1, no. 1, pp. 76–94, 1971.

[38] T. Achterberg, T. Koch, and A. Martin, "Branching rules revisited," *Oper. Res. Lett.*, vol. 33, no. 1, pp. 42–54, 2005.

[39] R. Christie, "118 Bus Power Flow Test Case," 1993. [Online]. Available: http://labs.ece.uw.edu/pstca/pf118/pg_tca118bus.htm. [Accessed: 22-Jan-2020].

[40] JEAS, "24-hour IEEE 118-bus system," 2021. [Online]. Available: http://motor.ece.iit.edu/Data/JEAS_IEEE118.doc. [Accessed: 11-Jan-2021]

[41] E. A. Belati, C. F. Nascimento, A. B. Dietrich, and H. De Faria Jr., "Sensitivity analysis applied to nodal technical losses evaluation in power transmission systems," *Int. Trans. Electr. Energy Syst.*, vol. 24, no. 2, 2014

[42] E. Reyes-Archundia, J. A Gutiérrez-Gnecchi, and A. Méndez-Patiño, A., "Impact of TCSC on directionality of traveling waves to locate faults in transmission lines, " *IEEE Latin America Transactions*, 19(1), 147–154, 2021

[43] B. Liu, Q. Yang, H. Zhang and H. Wu, "An interior-point solver for AC optimal power flow considering variable impedance-based FACTS Devices," *IEEE Access*, vol. 9, pp. 154460-154470, 2021.

Jacqueline S. Pereira received the BSc. degree in electrical engineering from UNIFEI (2013), and MSc. from UFABC (2017). She worked at ABB Brazil with Power Quality Solutions, and currently she is an Engineer at Ramboll, in Denmark.

Edmarcio A. Belati holds a master's degree from UNESP (1998) and a doctorate from USP (2003) in Electrical Engineering. He has experience in using optimization techniques applied to Electric Power Systems. He is currently a professor at UFABC.

Claudionor F. do Nascimento received the B.Sc. degree in electrical engineering from UNESP (1992), the M.Sc. and the Ph.D. degrees in electrical engineering from USP, in 2003 and 2007, respectively. He is an Associate Professor at UFSCar.

Paulo F. Silva was born in 1995 in the city of São Carlos, SP, Brazil. He is currently pursuing an academic master's degree in the Postgraduate Program in Electrical Engineering at the Federal University of São Carlos (PPGEE/UFSCar).

Priscila Rossoni has a degree in Computer Engineering from Centro Universitário Fundação Santo André (2013). She has a master's degree in Electrical Engineering from UFABC. She is currently a PhD student in Energy at UFABC.